Manipulating Nanoparticles in Solution with Electrically Contacted Nanotubes Using Dielectrophoresis

Lifeng Zheng,† Shengdong Li,† James P. Brody,†,‡ and Peter J. Burke*,†,‡

Department of Electrical Engineering and Computer Science and Biomedical Engineering, University of California, Irvine, California 92697

Received February 4, 2004. In Final Form: July 13, 2004

Dielectrophoresis is an electronic analogue[1,2] of optical tweezers[3] based on the same physical principle: an ac electric field induces a dipole moment on an object in solution, which then experiences a force proportional to the gradient of the field intensity. For both types of tweezers, this force must compete with thermal Brownian[4] motion to be effective, which becomes increasingly difficult as the particle size approaches the nanometer scale. Here we show that this restriction can be overcome by using the large electric field gradient in the vicinity of a carbon nanotube to electronically manipulate nanoparticles down to 2 nm in diameter.

I. Introduction

The physical principles of self-assembly that give rise to complicated three-dimensional structures on the nanometer scale in both biological and synthetic systems have been studied extensively.[5,6] The forces at work include noncovalent inter- and intramolecular interactions, i.e., hydrogen bonding, van der Waals, metal−ligand interactions, $\pi-\pi$ stacking, and hydrophobic vs hydrophilic interactions. These bottom−up principles of self-assembly, while efficient and economical, generally are passive; i.e., they are controlled only by macroscopic quantities such as temperature, pH, and solvent concentration. It would be a distinct advantage if this assembly process could be actively, electronically controlled, especially with nanometer spatial resolution. In this regard, top−down approaches to the manipulation of matter have been successful at the nanometer scale only with atomic force microscopy (AFM)/scanned probed technologies, which are difficult to scale to a massively parallel environment, such as that envisioned in the nascent field of molecular electronics.

In a separate, related research theme, the use of electric fields generated by an external voltage source to actively manipulate the locations of nanometer scale objects and large molecules such as DNA and proteins is well-known from conventional, established techniques such as gel electrophoresis. Here, the electrodes used are typically macroscopic in size, i.e., many centimeters. A recent variant on this research theme is the integration of microelectronic fabrication techniques such as photolithography to fabricate electrodes with dimensions on the order of millimeters or hundreds of micrometers.[7,8] In these electrophoresis techniques, charged species respond via the Coulomb force to dc electric fields. As a result, a limitation of the technique is that neutral species are unaffected and hence cannot be manipulated.

One available technique to electronically manipulate the position of both neutral and charged species in solution is to use ac electric fields, a technique called dielectrophoresis.[1] The physical principles of dielectrophoresis are well-established. If a polarizable object is placed in an electric field, there will be an induced positive charge on one side of the object and an induced negative charge (of the same magnitude as the induced positive charge) on the other side of the object. The positive charge will experience a pulling force; the negative charge will experience a pushing force. However, in a nonuniform field, the electric field will be stronger on one side of the object and weaker on the other side of the object. Hence, the pulling and pushing forces will not cancel, and there will be a net force on the object. This is the dielectrophoresis (DEP) force.

The key physical insight in this paper is that we use carbon nanotubes *as the electrode* to generate the electric field gradient; the nanotubes are electrically contacted by lithographically defined metal electrodes, which are far away from the region of interest, so that the fields from the metal electrodes are numerically insignificant compared to the fields generated by the nanotube itself. Since the electric field gradient in the vicinity of a nanotube is large, nanoparticles as small as 2 nm in diameter can be manipulated despite the large tendency for random, thermal Brownian motion important for such small particles. This is an order of magnitude smaller than previous nanoparticles that were manipulated with lithographically defined electrodes, and represents the first use of nanotube electrodes in dielectrophoresis. Because this allows an electronic link to the nanometer world, this technology may find applications as a component of massively parallel, actively controlled nanomanufacturing platforms and, generally speaking, may provide a bridge between top−down and bottom−up approaches to nanotechnology.

* To whom correspondence may be addressed. E-mail: pburke@uci.edu.

† Department of Electrical Engineering and Computer Science.

‡ Biomedical Engineering.

(1) Pohl, H. A. *Dielectrophoresis*: *The Behavior of Neutral Matter in Nonuniform Electric Fields*; Cambridge University Press: Cambridge, 1978.

(2) Burke, P. J. Nanodielectrophoresis: Electronic Nanotweezers. In *Encyclopedia of Nanoscience and Nanotechnology*; Nalwa, H. S., Ed.; American Scientific: Stevenson Ranch, CA, 2004.

(3) Ashkin, A.; Dziedzic, J. M.; Bjorkholm, J. E.; Chu, S. *Opt. Lett.* **1986**, *11*, 288−290.

(4) Einstein, A. *Ann. Phys.* **1905**, *17*, 549−560.

(5) Whitesides, G. M.; Mathias, J. P.; Seto, C. T. *Science* **1991**, *254*, 1312−1319.

(6) Philp, D.; Stoddart, J. F. *Angew. Chem., Int. Ed. Engl.* **1996**, *35*, 1155−1196.

(7) Cheng, J.; Sheldon, E. L.; Wu, L.; Uribe, A.; Gerrue, L. O.; Carrino, J.; Heller, M. J.; O'Connell, J. P. *Nat. Biotechnol.* **1998**, *16*, 541−546.

(8) Huang, Y.; Ewalt, K. L.; Tirado, M.; Haigis, T. R.; Forster, A.; Ackley, D.; Heller, M. J.; O'Connell, J. P.; Krihak, M. *Anal. Chem.* **2001**, *73*, 1549−1559.

10.1021/la049687h CCC: $27.50
Published on Web 08/24/2004

II. Theoretical Background

II.1. Quantitative Force Predictions. In an electric field $\vec{E}$, a dielectric particle behaves as an effective dipole with (induced) dipole moment $\vec{p}$ proportional to the electric field, i.e.

$$\vec{p} \propto \vec{E} \tag{1}$$

The constant of proportionality depends in general on the geometry of the dielectric particle. In the presence of an electric field gradient, the force on a dipole is given by

$$\vec{F} = (\vec{p}\cdot\vec{\nabla})\vec{E} \tag{2}$$

Combining the two equations, using known results for the relationship between $\vec{p}$ and $\vec{E}$ for a spherical particle of radius r and dielectric constant ϵ_p, and taking into account the liquid (medium) dielectric constant ϵ_m, it can be shown that the force acting on a spherical particle (the *dielectrophoresis* force) is given by[1,9]

$$\vec{F}_{DEP} = 2\pi v \epsilon_m K(\omega)\vec{\nabla}(\vec{E}_{rms}{}^2) \tag{3}$$

where v is the volume of the particle, $\vec{E}_{rms}$ is the root mean square (rms) value of the electric field (assuming a sinusoidal time dependence), and $K(\omega)$ is the real part of what is called the Clausius−Mosotti factor, which is related to the particle dielectric constant ϵ_p and medium dielectric constant ϵ_m by

$$K(\omega) \equiv \mathrm{Re}\left[\frac{\epsilon_p{}^* - \epsilon_m{}^*}{\epsilon_p{}^* + 2\epsilon_m{}^*}\right] \tag{4}$$

Here the asterisk (*) denotes that the dielectric constant is a complex quantity, and it can be related to the conductivity σ and the angular frequency ω through the standard formula

$$\epsilon^* \equiv \epsilon - i\frac{\sigma}{\omega} \tag{5}$$

When appropriately applied, eq 5 also takes into account surface conductances[10] of the particles and the electrical double layer formed at the interface between the particle and the medium.

II.2. Frequency Dependence. For spherical particles, the Clausius−Mosotti factor $K(\omega)$ can vary between −0.5 and +1.0. When it is positive, particles move toward higher electric field regions, and this is termed positive dielectrophoresis. When it is negative, the particles move toward smaller electric field regions, and this is termed negative dielectrophoresis. Since $K(\omega)$ is frequency dependent, both positive and negative DEP can be observed in the same system by varying the frequency.

II.3. Brownian Motion. In addition to DEP forces, small particles also undergo thermal Brownian motion.[4] This can be treated as an effective random force whose maximum value is given roughly by

$$F_{thermal} = k_B T/v^{1/3} \tag{6}$$

where k_B is the Boltzmann constant, T is the temperature, and v is the particle volume. In general, there are two regimes of operation for DEP: First, when DEP forces exceed the thermal force. In this case the motion is determined primarily by the DEP force with small, random deviations. In the second case, where the Brownian motion dominates, the particle trajectory is mostly random, with a small tendency to move in the direction of the DEP force. According to eq 3, the DEP force for a spherical particle scales as the radius cubed, whereas according to eq 6 the thermal force scales as the inverse radius. Therefore, for very small particles, the thermal force will dominate. As eq 3 shows, the DEP force depends primarily on the particle size and the gradient of the electric field intensity. The field gradient is determined by the electrode geometry, which we now discuss; it is the prime focus of our paper.

II.4. Electrode Geometry. What generates the electric field and, more importantly, the electric field gradient quantified in eq 3? Generally, this is achieved by two metal electrodes with an applied ac voltage. In this case, the order of magnitude of the electric field is set by the applied voltage divided by the spacing between the electrodes. The *gradient* is more sensitive to the details of the electrode geometry.

Historically,[1] the use and study of dielectrophoresis was between a sharp pin and a flat surface, because that is the easiest geometry in which one can create a strong field gradient, hence a strong dielectrophoretic force. From this geometry, assuming a 500 μm radius for the tip of the pin, 5000 V for the applied voltage, and 1 mm for the particle distance from the electrode, Pohl predicted that for particles smaller than 500 nm the DEP force would be negligible compared to Brownian motion.[1]

Since the advent of optical and then electron-beam lithography, the use of microfabricated planar metal electrodes on insulating substrates has achieved much more attention, since it allows many different flexible geometries to be designed, tested, and used. Moreover, by using small gaps between electrodes, large electric field strengths can be achieved, thus further increasing (in general) the achievable dielectrophoretic force.

The manipulation of spherical nanoparticles down to about 15 nm has been achieved using lithographically defined electrodes, including both metallic and insulating nanoparticles. (A recent review contains exhaustive references to the scholarly literature covering the manipulation of nanoparticles with lithographically defined electrodes.[2]) Nanoparticles smaller than this have not been manipulated because, even with lithographically fabricated electrodes, the field gradients are not large enough to allow the magnitude of the DEP force to overcome thermal motion for nanoparticles smaller than about 15 nm in diameter.

II.5. DEP Forces on Prolate Objects. We turn next to the discussion of prolate objects. Equation 3 applies to spherical particles, but it is well-known that long, thin objects have enhanced polarizability. For DEP, this means that objects with a few nanometers of diameter that are of order micrometers in length can still be manipulated by electrical field gradients generated by lithographically fabricated electrodes. Three interesting cases are DNA, nanotubes, and nanowires. Experimentally, it has been possible to align these objects with DEP and then cause them to bridge the gap between two lithographically fabricated electrodes, thus making electrical contact. Although extensive research has been performed on the manipulation of DNA,[13] nanotubes,[14−25] and nanowires[26−28]

(9) Jones, T. B. *Electromechanics of particles*; Cambridge University Press: Cambridge, 1995.
(10) Morgan, H.; Green, N. G. *AC electrokinetics*: *colloids and nanoparticles*; Research Studies Press, Ltd.: Baldock, Hertfordshire, England, 2003.
(11) Wang, X. J.; Wang, X. B.; Becker, F. F.; Gascoyne, P. R. C. *J. Phys. D*: *Appl. Phys.* **1996**, *29*, 1649−1660.
(12) Clague, D. S.; Wheeler, E. K. *Phys. Rev. E* **2001**, *6402*, art. no. 026605.

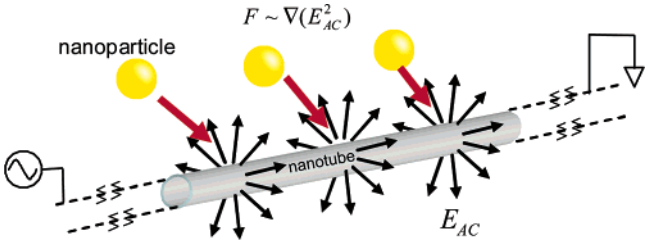

Figure 1. Schematic geometry showing the electrically contacted nanotube as the electrode. Except near the ends (which are usually covered by thin film electrodes), the nanoparticles experience an inward radial force toward the surface of the nanotube.

using electric fields generated from lithographically fabricated metal electrodes, that is specifically *not* the topic of this paper, as we discuss next.

II.6. Carbon Nanotubes as Electrodes. All DEP studies to date have used lithographically fabricated metal electrodes to generate the electric field gradients and, therefore, have been limited as to the smallest particle size they can manipulate. The key physical insight in this paper is that we use carbon nanotubes *as the electrode* to generate the electric field gradient; the nanotubes are electrically contacted by lithographically defined metal electrodes. Hence, in this work we are able to manipulate nanoparticles with nanoelectrodes down to 2 nm in diameter using dielectrophoresis, an order of magnitude smaller than previous nanoparticles that were manipulated. A schematic diagram indicating this principle is shown in Figure 1.

III. Experimental Methods

III.1. Sample Fabrication. The carbon nanotubes were grown with chemical vapor deposition from lithographically defined catalyst sites, after Kong.[29] Using conventional photolithography, we fabricate wells directly in photoresist (Shipley 1827) on a 4 in. oxidized (300 nm) silicon wafer (100, n-type, resistivity 5−10 Ω cm) or onto quartz slides. Next, 2.0 g of alumina nanoparticles (Degussa, aluminum oxide C), 2.5 mmol of $Fe(NO_3)_3 \cdot 9H_2O$ (Aldrich), and 0.7 mmol of $MoO_2(acac)_2$ (Aldrich) are added to 60 mL of deionized (DI) water in sequence while violently stirring. Since the $Fe(NO_3)_3$ is soluble in water, spinning this solution directly onto the wafer would remove most of the Fe. This would be an undesirable consequence, since the Fe plays a crucial catalytic role in the nanotube growth. To alleviate this problem, 15 mL of ammonia (concentrate) was slowly dropped into the mixture from above. This caused the formation of $Fe(OH)_3$, which precipitates. The mixture was stirred for 24 h followed by sonication for 3 h, resulting in a suspension of 1.25 mmol Fe_2O_3/0.7 mmol MoO_3/2.0 g alumina and water. Two drops of this suspension were deposited onto the patterned photoresist. After spinning on the suspension at 3400 rpm for 40 s, and after a 100 °C for 20 min bake, lift-off of the photoresist in acetone led to the final sample with catalyst pattern ready to carry out chemical vapor deposition (CVD).

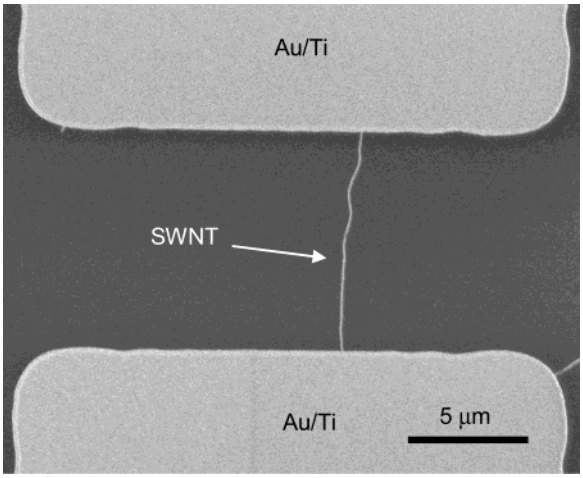

Figure 2. SEM image of typical nanotube contacted electrically with Au/Ti bilayer, before the DEP experiments.

CVD was carried out using a 3 in. Lindberg furnace. A gas recipe that favors the synthesis of ultralong and high-quality single-walled nanotubes (SWNTs) was adopted in the experiment. After heating up the 3 in. quartz tube to 900 °C under an argon atmosphere, the argon was replaced by a coflow of 1000 sccm methane (99.999%) and 200 sccm hydrogen for 12 min. All the processes were performed under manual control, including purging Ar, increasing the temperature, flowing active gases, and cooling the system in the Ar atmosphere again. After CVD, we find our nanotubes are strongly van der Waals bound to the surface, and stay that way for the rest of the sample preparation and DEP experiments. To be clear, *in contrast to previous work where metal electrodes were used to manipulate nanotubes freely suspended in solution (see II.5), our nanotubes are firmly bound to the surface and do not move during the entire course of the experiments.*

As-obtained samples were characterized by a scanning electron microscope (Hitachi S-4700) using beam energies of 1 keV. Typical nanotube lengths were between 1 and 50 μm in length. AFM images of growth results show that the diameter of as-grown nanotubes is less than 1.5 nm. Thus we infer that the nanotubes grown from the nanoparticle catalysts are single walled nanotubes.

After the location of the nanotubes with respect to the catalyst pads was determined under SEM, optical lithography was used to electrically contact the nanotubes using thermal or electron-beam evaporation of 10 nm Ti/100 nm Au and liftoff. The catalyst pads were used as optical alignment marks. The electrode geometry included a 5−10 μm gap between two Au electrodes. Each Au/Ti electrode was electrically contacted with a 25 μm gold wire using bond pads ~1 mm^2 located approximately 1 cm away from the gap. Figure 2 shows an SEM image of a sample after electrical contact. In some cases, more than one nanotube was contacted on both ends. In other cases, a nanotube would be contacted by one electrode but not the other. Additionally, there were cases where nanotubes were near the electrodes, but

(13) Zheng, L.; Brody, J. P.; Burke, P. J. *Biosens. Bioelectron.*, in press, and references therein.
(14) Bezryadin, A.; Dekker: C. *J. Vac. Sci. Technol., B* **1997**, *15*, 793−799.
(15) Yamamoto, K.; Akita, S.; Nakayama, Y. *Jpn. J. Appl. Phys. 2* **1996**, *35*, L917−L918.
(16) Wakaya, F.; Nagai, T.; Gamo, K. *Microelectron. Eng.* **2002**, *63*, 27−31.
(17) Chen, X. Q.; Saito, T.; Yamada, H.; Matsushige, K. *Appl. Phys. Lett.* **2001**, *78*, 3714−3716.
(18) Yamamoto, K.; Akita, S.; Nakayama, Y. *J. Phys. D*: *Appl. Phys.* **1998**, *31*, L34-L36.
(19) Bubke, K.; Gnewuch, H.; Hempstead, M.; Hammer, J.; Green, M. L. H. *Appl. Phys. Lett.* **1997**, *71*, 1906−1908.
(20) Krupke, R.; Hennrich, F.; Weber, H. B.; Kappes, M. M.; von Lohneysen, H. *Nano Lett.* **2003**, *3*, 1019−1023.
(21) Krupke, R.; Hennrich, F.; Weber, H. B.; Beckmann, D.; Hampe, O.; Malik, S.; Kappes, M. M.; Lohneysen, H. V. *Appl. Phys. A*: *Mater. Sci. Process.* **2003**, *76*, 397−400.
(22) Nagahara, L. A.; Amlani, I.; Lewenstein, J.; Tsui, R. K. *Appl. Phys. Lett.* **2002**, *80*, 3826−3828.
(23) Chung, J. H.; Lee, K. H.; Lee, J. H. *Nano Lett.* **2003**, *3*, 1029−1031.
(24) Kumar, M. S.; Lee, S. H.; Kim, T. Y.; Kim, T. H.; Song, S. M.; Yang, J. W.; Nahm, K. S.; Suh, E. K. *Solid State Electron.* **2003**, *47*, 2075−2080.
(25) Chung, J. Y.; Lee, K. H.; Lee, J. H.; Ruoff, R. S. *Langmuir* **2004**, *20*, 3011−3017.
(26) van der Zande, B. M. I.; Koper, G. J. M.; Lekkerkerker, H. N. W. *J. Phys. Chem. B* **1999**, *103*, 5754−5760.
(27) Smith, P. A.; Nordquist, C. D.; Jackson, T. N.; Mayer, T. S.; Martin, B. R.; Mbindyo, J.; Mallouk, T. E. *Appl. Phys. Lett.* **2000**, *77*, 1399−1401.
(28) Huang, Y.; Duan, X. F.; Wei, Q. Q.; Lieber, C. M. *Science* **2001**, *291*, 630−633.
(29) Kong, J.; Soh, H. T.; Cassell, A. M.; Quate, C. F.; Dai, H. J. *Nature* **1998**, *395*, 878−881.

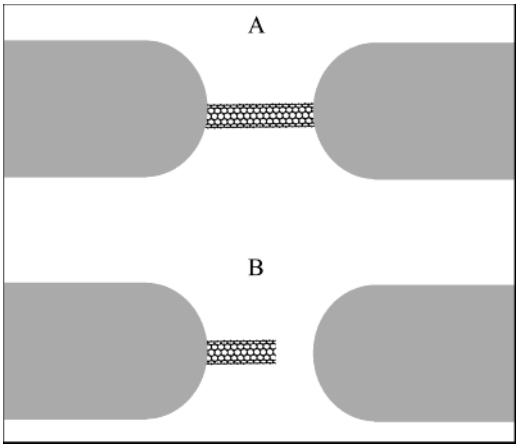

Figure 3. Schematic of electrode geometry for studies presented in this paper: (A) nanotube electrically contacted on both ends; (B) nanotube electrically contacted on one end only. For this case, the nanotube may point in a random direction.

not contacted at all. Some typical cases are indicated schematically in Figure 3.

III.2. Nanoparticle Suspensions. Two types of nanoparticles suspensions were used in this work: polystyrene nanoparticles of diameters 20 and 100 nm, and Au nanoparticles of diameters 2 and 10 nm. For the polystyrene nanoparticles, suspensions of commercially available (Molecular Probes, Inc.) carboxylate-modified, fluorescently labeled polystyrene nanoparticles (d = 20 nm or 100 nm) were diluted 10^4 times with DI water (18 MΩ cm) to a density of approximately 10^{11} particles/mL. (The as-purchased nanoparticles were suspended in 2 mM sodium azide; the sodium azide was thus also diluted to 200 nM.) For the Au nanoparticles, suspensions of commercially available (Ted Pella, Inc.) colloidal Au (d = 2 or 10 nm) were diluted 10^9 times with DI water (18 MΩ cm) to a density of approximately 10^5 particles/mL. No electrolyte was used in either suspension.

III.3. Experimental Protocol. In our experiments, electrical connection to the nanotubes is achieved by evaporated Au/Ti electrodes as described in section III.1. Samples were rinsed in methanol and DI water before the experiments. Au wires are soldered to the Au/Ti electrodes with In solder and then connected to a function generator (Stanford Research Systems, model DS 345). An aliquot of suspension (6 μL) is dropped onto the chip containing the electrically contacted single-walled carbon nanotubes. The implications of this geometry on the electric field distribution will be discussed in the next section.

Several protocols were tested to see if they were suitable for DEP manipulation. All protocols involved the application of an ac voltage to one gold electrode after dropping the aliquot onto the sample, while the other gold electrode was grounded. The aliquot covered the nanotubes and part of the gold electrodes. In some experiments the sample was allowed to dry in air while the ac voltage was applied. In some experiments, a cover slip was used and the solution was allowed to dry while the ac voltage was applied. In some experiments, the ac voltage was turned off before the solution dried, and a DI water rinse was applied, which was then allowed to dry.

A sinusoidal ac voltage is applied at 500 kHz for the polystyrene nanoparticles and 500 kHz to 10 MHz for the Au nanoparticles, both with amplitude of 4−20 V_{pp}. The frequency was chosen low enough to be in the positive DEP region but high enough so that electrolysis would not occur. Prior experiments in our lab on DEP manipulation of polystyrene nanoparticles using lithographically fabricated gold electrodes found a crossover from positive to negative DEP at 5 MHz for 100 nm nanoparticles, and 20 MHz for 20 nm nanoparticles,[13] so that our experiments should be in the positive DEP region. This means the particles will be attracted to regions of highest field intensity. As we discuss below, this is at the surface of the nanotube. During the experiments, the ac current was not measured but can be estimated. Typical resistances of nanotubes for this work are on the order of 100 kΩ to 1 MΩ, so that the current flowing through the nanotube is of order 10 μA. Since the suspending solution was DI water, the ac electrical current flowing through the colloidal suspension is assumed to be negligible.

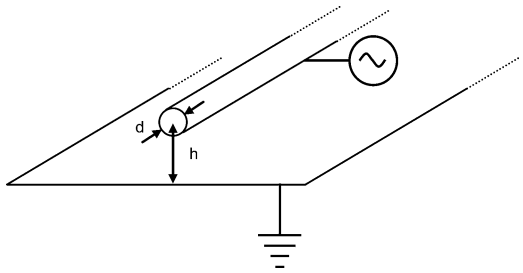

Figure 4. Model geometry for cylinder above a ground plane. In practice there is a dielectric (oxide) between the nanotube and the conducting Si substrate.

In some experiments where quartz was used as the substrate, the sample was imaged through an inverted Nikon TE200 microscope, equipped with a 20×/0.4 NA objective. This was done during the application of the ac voltage. Fluorescent images used epi-illumination with a mercury arc lamp providing the excitation. A Nikon Coolpix 995 camera captured the images.

III.4. Post-DEP Characterization Techniques. After DEP manipulations, the samples were characterized in either a SEM (Hitachi S-4700) or an AFM (Digital Instruments, Multimode) in tapping mode. SEM imaging on insulating substrates (such as quartz) can be complicated by substrate charging effects. Therefore, for some samples, a thin layer (10 nm) of Au is sputtered onto the sample to enhance the SEM image contrast.

III.5. Electric Field Distribution. Since our nanotubes are several micrometers long, most nanoparticles will be very far from the ends of the nanotube compared to the size of the nanoparticle and the diameter of the nanotube. For this reason, we focus mainly on the electric field distribution for positions very far from the ends of the nanotubes. In this case, the electric field direction will be primarily radial, as will the direction of the gradient and hence DEP force. Effects of the nanotube ends will be discussed later in this section. Therefore, most nanoparticles experience a predominantly *inward radial force*, independent of the position along the nanotube.

To estimate the magnitude of the DEP force, it is necessary to know the electric field distribution, especially the gradient. In this paper, we focus on using physical insight and model geometries. This allows estimates of scaling laws and semi-quantitative force calculations. Figure 4 shows the geometry of interest. For the purposes of this paper we model the nanotube as a metal wire with diameter of 1 nm. While nanotubes are not perfect metals, this approximation is sufficient to approximate the spatial electric field distribution.

The boundary condition at the surface of a metal is that the electric field is perpendicular to the surface. This means the fields at the surface of a nanotube (in our toy model) will point radially. To understand from a qualitative perspective the field gradients in the vicinity of a nanotube, we consider Figure 4 in more detail. This geometry is appropriate for our experiments performed on oxidized Si wafers. Since the Si wafer is doped, it can be considered a good conductor, hence an equipotential (i.e., a ground plane). The distance from the nanotube to the doped Si is about 300 nm, whereas the nanotube diameter is about 1 nm. Therefore, we can consider the limit where $h \gg d$. In this case, and when the nanotube length is much larger than h, the radial electric field close to the nanotube is given approximately by

$$\vec{E}_{\mathrm{rms}} \approx \frac{V_{\mathrm{rms}}}{\ln(4h/d)} \frac{1}{r} \hat{r} \tag{7}$$

where V_{rms} is the rms ac voltage applied to the nanotube, r is the radial distance away from the center of the nanotube, and $\hat{r}$ is a unit vector pointing in the radial direction. From this, we can calculate the gradient of the electric field squared, finding

$$\vec{\nabla}({E_{\mathrm{rms}}}^2) \approx -2\left(\frac{V_{\mathrm{rms}}}{\ln(4h/d)}\right)^2 \frac{1}{r^3} \hat{r} \tag{8}$$

The key point of this paper is that, because the field gradient and hence DEP force scale as $1/r^3$, and because r can be in the nanometer regime when carbon nanotubes are used as electrodes, the DEP force can overcome Brownian motion even for the smallest of nanoparticles.

On the basis of this simple calculation, for an applied voltage of 1 V, the DEP force at the surface of the nanotube experienced by a 1 nm dielectric particle (taking $r = 0.5$ nm, d = 1 nm, $h =$ 300 nm) can be estimated using eq 3 as ~100 pN, whereas the effective thermal Brownian motion random force for a 1 nm particle from eq 6 can be estimated as ~1 pN. This simple calculation, then, predicts that the DEP forces on even the smallest of nanoparticles should be larger than the thermal motion effective force if nanotubes are used as the electrodes.

The above calculations should be taken as estimates only, which use classical electromagnetics to estimate the behavior of electrical nanosystems. For example, for an applied voltage of 1 V on the nanotube, eq 7 predicts an electric field of order 10^7 V/m, which is quite large. Other physical effects probably are important in the nanometer scale, which will cause the real electric field to be less than this value. While these other effects are currently not clearly understood, our work described below demonstrates that the simple physical insight of using nanotubes as electrodes does indeed work experimentally.

For the nanotubes electrically contacted at one end, the ac voltage was applied to the electrode connected to the nanotube. Since very little current flows into the nanotube, the voltage drop along the length of the nanotube is negligible. Therefore, the circuit model shown in Figure 4 is valid along the entire length of the nanotube, except near the ends. For nanotubes which are electrically contacted at both ends, since our nanotubes are several micrometers long, and probably somewhat resistive compared to the gold electrodes, the local voltage between the nanotube and the substrate will vary along the length of the nanotube. At the nanotube end closest to the grounded gold electrode, the voltage on the nanotube with respect to ground will be zero. On the other hand, at the nanotube end closest to the electrode with the voltage applied, the nanotube−ground plane voltage difference will be largest. Very close to the gold electrodes (on a scale compared to *d*), the electrical fields will deviate significantly from eq 7. However, for most of the nanotube length in our experiments, eq 7 is a good approximation.

Some of our samples were fabricated on a quartz wafer, which can be considered insulating, so that Figure 4 is not appropriate. In that case, the electric field distribution is not as simple to calculate. However, it is still the case that, near the surface of the nanotube, the electrical field is perpendicular to the nanotube and that the gradient (hence DEP) force should be very large. Our experiments bear out this claim.

There will also be large gradients near the ends of the tubes, which will cause DEP forces there, as well. The very tip of the nanotube will have strong field gradients as well, and similar arguments could be given that the tips could be used to trap nanoparticles. At least one end of the nanotubes in our work is usually covered with Au thin films, but in cases where an end is exposed, we do see trapping of nanoparticles both at the ends and along the length of the nanotubes.

IV Results and Discussion

IV.1. Polystyrene Nanoparticles. Twenty six separate experiments were performed on DEP manipulation of Polystyrene nanoparticles, of which about 25% of them showed clearly attached polystyrene nanoparticles under SEM characterization after drying. We found experimentally that the nanoparticles are present under SEM independent of whether the cover slip was on or off during drying. Additionally, the results were independent of whether a post-DEP rinse in DI water was performed. The results were also independent of the substrate used, showing similar results on both quartz and oxidized Si wafers. In addition, in control experiments where no ac voltage was applied, we never observed the attachment of nanoparticles to nanotubes. Taken collectively, these results lead us to conclude that the ac electric fields are indeed causing the nanoparticles to come into intimate contact with the nanotubes and that they remain attached to the nanotubes even after DI water rinse, solution drying, and exposure to the vacuum environment of an SEM.

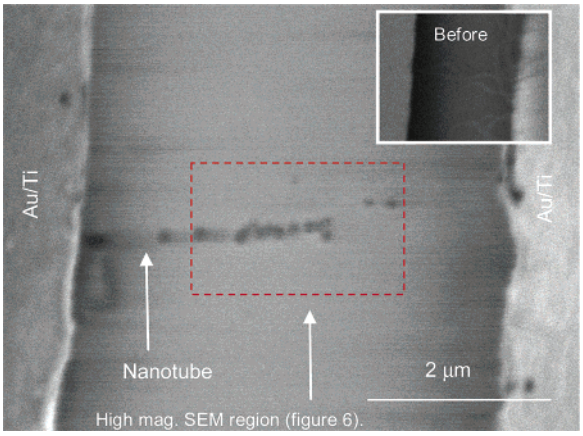

Figure 5. SEM images of nanotube contacted electrically on both ends, before and after the trapping experiments using 100 nm polystyrene nanoparticles. The alignment along the tubes is clear.

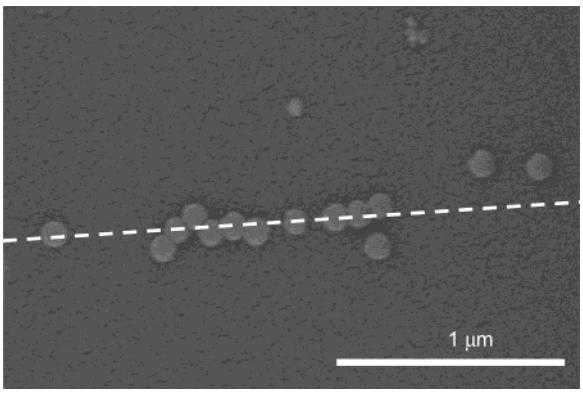

Figure 6. High magnification image of region outlined in Figure 5, after Au has been sputtered to enhance resolution and contrast of the 100 nm nanoparticles. The dashed white line shows where the nanotube is, which is not visible because it is covered by 10 nm of sputtered Au.

In Figure 5, we show an SEM image of a nanotube on a quartz wafer both before and after the DEP experiment. This is an example of a nanotube contacted electrically on both ends. The trapped 100 nm nanoparticles are clearly visible preferentially attached along the length of the nanotube, forming a "pearl chain". To allow clearer SEM images, Au was sputtered uniformly onto the entire sample (including the electrodes, nanotube, and attached nanoparticles) and imaged more carefully under SEM. This image is shown in Figure 6.

In some experiments, the nanotube was electrically contacted on one end only. In this case, we were also clearly able to see preferential attachment of the nanoparticles to the nanotube. In Figure 7, we show a series of images indicating the process. Figure 7a shows an image of the nanotubes and gold electrodes before the DEP experiments. Figure 7b shows fluorescence microscopy images taken during the DEP experiment. It clearly shows that the nanoparticles were attached to the nanotubes during the DEP experiment before the solution dried. (In this experiment, both 20 and 100 nm nanoparticles were used.) Figure 7c shows an SEM image, which indicates the nanoparticles are still attached to the nanotubes, even after the solution dries. To more clearly see this, we show in Figures 8 and 9 higher magnification SEM images of

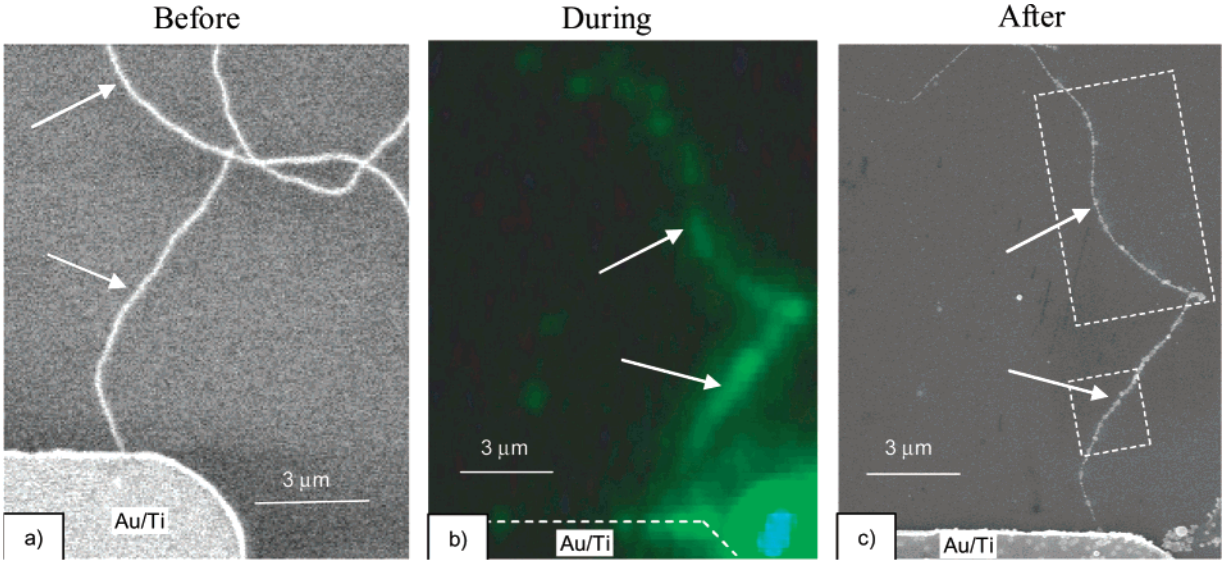

Figure 7. Key result of this paper: (A) SEM image of the nanotubes and gold electrodes before the DEP experiments; (B) fluorescence microscopy images taken during the DEP experiment (the solution was still on the sample.); (C) SEM image of the nanoparticles attached to the nanotubes after the DEP experiments.

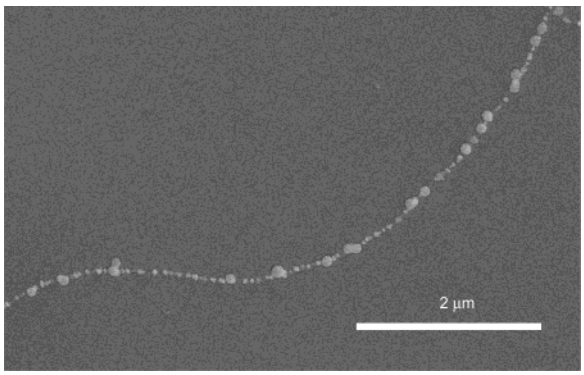

Figure 8. Zoom of Figure 7.

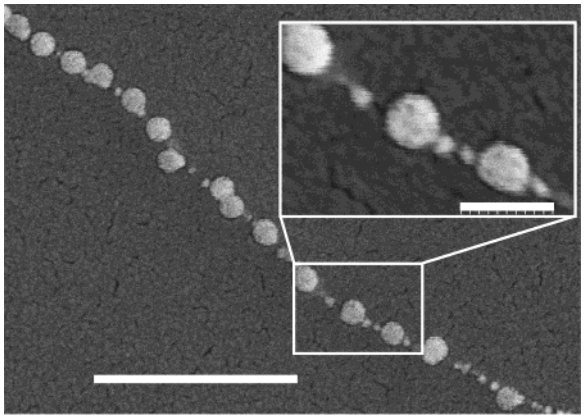

Figure 9. Another zoom of Figure 7: scale bar, 1 μm; scale bar inset, 200 nm. Both the 20 and 100 nm particles are clearly visible along the length of the nanotube.

the nanotube from Figure 7c, after sputtering Au onto the whole sample to increase the contrast. The attachment of the nanoparticles to the nanotube is clear.

IV.2. Control Experiments and Capillary Forces. Several groups have recently investigated the role of capillary forces in self-assembly. Since the drying force of droplets can be used to make particle chains by self-assembly of microparticles and nanoparticles in grooves[30−36] (which is qualitatively different than our experiments which have no such grooves), we have

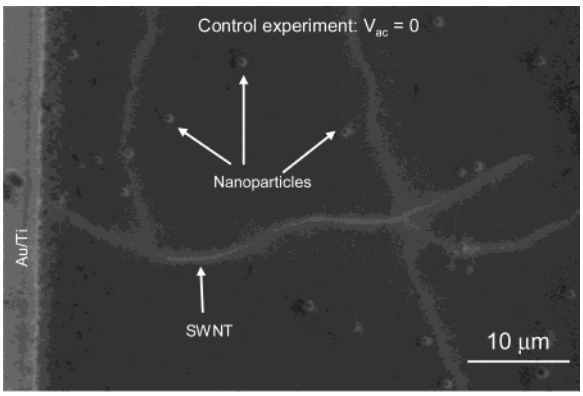

Figure 10. Control experiment in which no ac voltage was applied shows that nanoparticles do not attach to nanotubes.

investigated the possibility that capillary forces are at play in our experiments.

Several control experiments were performed to determine the role of capillary forces. First, as discussed above, experiments where no voltage was applied to the nanotubes never resulted in any preferential attachment of nanoparticles to the nanotubes. Figure 10 shows a typical SEM image of a control experiment where no ac voltage was applied. Nanoparticles and nanotubes are both clearly visible and not attached.

A separate indication that capillary forces are not responsible for the pearl chaining we observe comes from imaging of the fluorescently labeled nanoparticles performed during the application of the ac voltage, before the solution was allowed to dry. While the nanotubes are too small to be visible under an optical microscope, the electrodes were easy to see. Additionally, prior to the experiments, the location of the nanotubes was determined

(30) Xia, Y. N.; Yin, Y. D.; Lu, Y.; McLellan, J. *Adv. Funct. Mater.* **2003**, *13*, 907−918.
(31) Yin, Y. D.; Lu, Y.; Gates, B.; Xia, Y. N. *J. Am. Chem. Soc.* **2001**, *123*, 8718−8729.
(32) Yin, Y. D.; Xia, Y. N. *Adv. Mater.* **2001**, *13*, 267−271.
(33) Yin, Y. D.; Xia, Y. N. *J. Am. Chem. Soc.* **2003**, *125*, 2048−2049.
(34) Yin, Y. D.; Lu, Y.; Xia, Y. N. *J. Mater. Chem.* **2001**, *11*, 987−989.
(35) Gates, B.; Yin, Y. D.; Xia, Y. N. *J. Am. Chem. Soc.* **2000**, *122*, 12582−12583.
(36) Lu, Y.; Yin, Y. D.; Xia, Y. N. *Adv. Mater.* **2001**, *13*, 271−274.

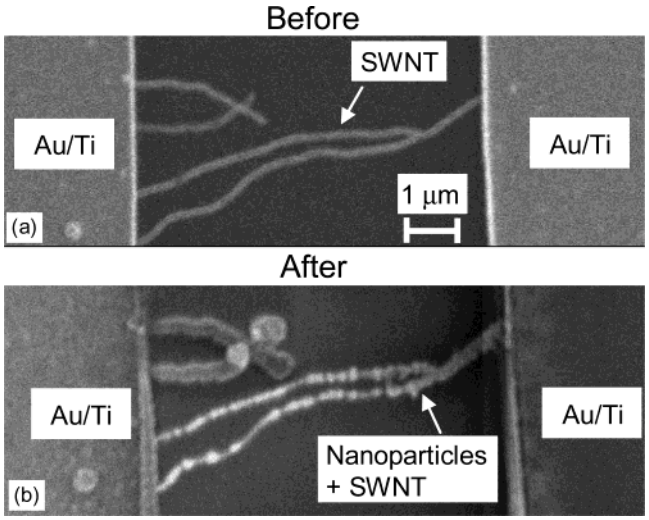

Figure 11. SEM image of nanotube contacted electrically on both ends before and after DEP experiments using 2 nm gold nanoparticles. The Au nanoparticles are attached to the nanotubes after the DEP experiments.

by SEM. Clear evidence for preferential attachment of the nanoparticles to the nanotube was clearly seen under fluorescence microscopy (see Figure 7).

Not all the nanoparticles in the solution are trapped at the surface of the nanotubes. To further investigate this issue, we performed control experiments by dropping a small aliquot on the corner of a sample, allowing it to dry, and characterizing the distribution of polystyrene nanoparticles after drying with SEM. We find the dominant population of polystyrene nanoparticles is at the edge of the aliquot that dried. This is due to capillary forces and surface tension moving the nanoparticles as the aliquot dries. However, the population of polystyrene nanoparticles in the original center of the aliquot was low (typically less than 100 nanoparticles per $100 \times 100\ \mu$m field of view of the SEM). This is similar to what happens to drops of coffee after drying on a table: Rings of dark regions are visible around the edges of the original drop.[37] Thus, since the polystyrene nanoparticle population in the center of the aliquot was not enhanced due to capillary forces after drying, and since the DEP experiments were performed with nanotubes in the center of the original aliquot, we are led to conclude that many of the nanoparticles that are not attached to the nanotube end up at the edge of the aliquot, which is far (several millimeters) away from the nanotube.

Taken collectively these control experiments lead us to conclude that capillary forces, while significant, are not responsible for the attachment of the nanoparticles to the nanotubes observed under SEM.

IV.3. Gold Nanoparticles. To test the scalability of the technique to smaller nanoparticles, we performed similar experiments with 2 and 10 nm Au nanoparticles. In Figure 11, we show an SEM image of electrically contacted nanotubes before and after the DEP experiments, where we used a sine wave at 1 MHz, amplitude 2 V_{pp}, and 2 nm Au nanoparticles. In this experiment, there are nanotubes contacted on both ends, as well as nanotubes contacted on only one end. Both types showed attached Au nanoparticles after the DEP experiments under SEM characterization. In two control experiments, an aliquot of Au nanoparticle solution was allowed to dry on a chip where no ac voltage was applied. In those

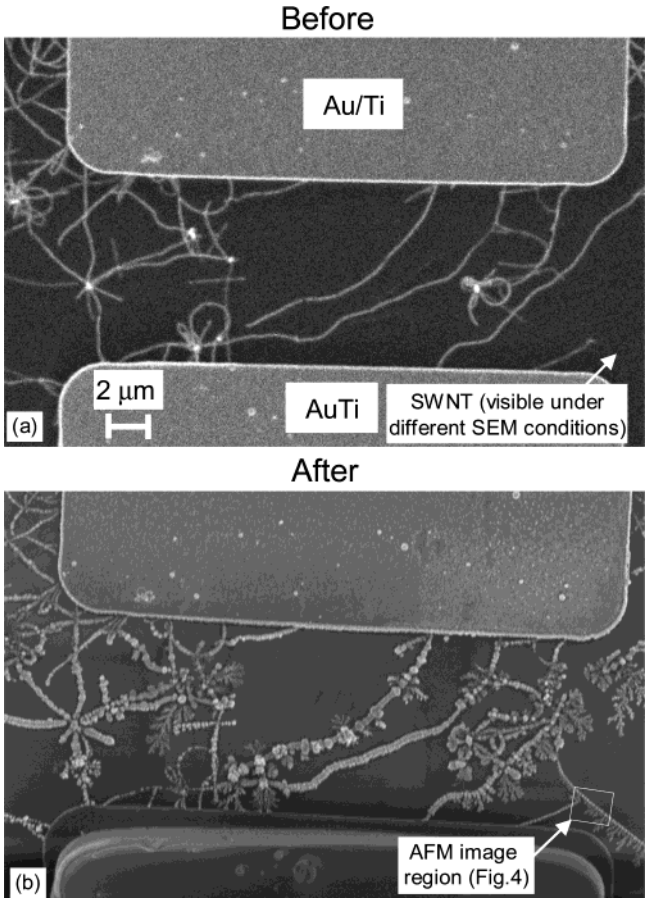

Figure 12. SEM images of SWNTs before and after DEP experiments.

experiments, we found no evidence that nanoparticles bind to the nanotube. Au nanoparticles of $d = 2$ nm were trapped in six of eight experiments with frequencies from 500 kHz to 10 MHz. Thus, the Au nanoparticle attachment to the nanotube is clearly controlled by the application of an ac voltage.

A more dramatic example of this Au nanoparticle trapping is shown in Figure 12. There, it is clear that the Au nanoparticles are dominantly attracted to the nanotubes. In addition, the gold nanoparticles form on the nanotubes regardless of whether they are straight or curled, whether they have kinks, or even where two nanotubes cross.

In Figure 12, it is interesting to note that a nanotube with Au nanoparticles is visible in the lower-right region of the image where there was no nanotube visible (via SEM) before. Under different SEM conditions, we indeed observe a nanotube where the nanoparticles were trapped. This is consistent with the work of Fuhrer,[38] who has clearly shown that SEM images of SWNTs are related closely to the detailed imaging conditions.

To more closely examine the morphology of the Au particles on the nanotubes, we present in Figure 13 an AFM image from a short section of one or our Au nanoparticle nanotubes. The tapping mode image (Figure 13a) clearly confirms dendritic growth off the side of some of the nanotubes. Similar dendritic growth has been studied by Velev[39,40] in complementary experiments using

(37) Deegan, R. D.; Bakajin, O.; Dupont, T. F.; Huber, G.; Nagel, S. R.; Witten, T. A. *Nature* **1997**, *389*, 827−829.

(38) Brintlinger, T.; Chen, Y. F.; Durkop, T.; Cobas, E.; Fuhrer, M. S.; Barry, J. D.; Melngailis, J. *Appl. Phys. Lett.* **2002**, *81*, 2454−2456.

(39) Bhatt, K. H.; Velev, O. D. *Langmuir* **2004**, *20*, 467−476.

(40) Hermanson, K. D.; Lumsdon, S. O.; Williams, J. P.; Kaler, E. W.; Velev, O. D. *Science* **2001**, *294*, 1082−1086.

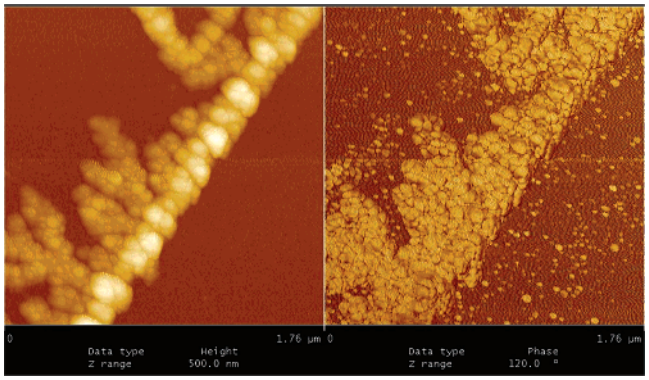

Figure 13. (left) Tapping mode and (right) phase contrast mode AFM images of a Au nanoparticles on a nanotube.

millimeter scale electrodes. The phase contrast image (Figure 13b) is more difficult to interpret physically but seems to indicate that if there are any nanoparticles that are not attached to the nanotube, the fraction is small.

IV.4. Discussion. In our experiments, we have clearly shown using a variety of techniques and control experiments that the application of an ac voltage to an electrically contacted nanotube in solution causes polystyrene nanoparticles (20 and 100 nm) and Au nanoparticles (2 and 10 nm) to be attached to the nanotubes. This attachment is strong enough to survive the capillary forces present on drying of the solution. We have demonstrated that the attachment of the nanoparticles is not a passive self-assembly process but rather an active, electronically controlled process.

At present, we do not know the type of bond that occurs at the attachment site. This is clearly a topic worthy of future study. An additional topic which we have not studied includes the effect of the nanotube electrical resistance and crystallographic properties. For example, do semiconducting and metallic nanotubes both give similar results when DEP trapping?

Finally, because the dielectric properties of the nanoparticles are frequency dependent, by varying the frequency, it should be possible to attract or repel nanoparticles; by using different species of nanoparticles, one could attract one species while repelling others. Multiple layers of shells could thus be built up on top of the nanotube. This is just one example of how this technique could be used for electronically controlled assembly of matter at the nanometer scale.

V. Conclusions

We have demonstrated, for the first time, the use of nanotube electrodes to manipulate nanoparticles in solution using dielectrophoresis. The technique should find broad applicability. In contrast to AFM-based nanofabrication techniques, this is purely electronic and hence requires no mechanical motion at either the nanoscale[41] or macroscale. Thus, the technique is inherently scalable for massively parallel nanomanipulation. In addition, it should be possible to manipulate biological nanostructures such as DNA,[13] viruses,[42] and proteins[43] using nanotube electrodes.

Acknowledgment. This work was supported by the Army Research Office (award DAAD19-02-1-0387), the Office of the Naval Research (award N00014-02-1-0456), and DARPA (award N66001-03-1-8914), and the National Science Foundation (award ECS-0300557).

LA049687H

(41) Kim, P.; Lieber, C. M. *Science* **1999**, *286*, 2148−2150.
(42) Morgan, H.; Hughes, M. P.; Green, N. G. *Biophys. J.* **1999**, *77*, 516−525.
(43) Washizu, M.; Suzuki, S.; Kurosawa, O.; Nishizaka, T.; Shinohara, T. *IEEE Trans. Ind. Gen. Appl.* **1994**, *30*, 835−843.